Accepted Manuscript

The long-term creep and shrinkage behaviors of green concrete designed for bridge girder using a densified mixture design algorithm

Trong-Phuoc Huynh, Chao-Lung Hwang, Andrian H. Limongan

PII: S0958-9465(17)30548-6

DOI: 10.1016/j.cemconcomp.2017.12.004

Reference: CECO 2958

To appear in: *Cement and Concrete Composites*

Received Date: 21 June 2017

Revised Date: 5 November 2017

Accepted Date: 5 December 2017

The long-term creep and shrinkage behaviors of green concrete designed for bridge girder using a densified mixture design algorithm

Trong-Phuoc Huynh[a,*], Chao-Lung Hwang[b], Andrian H. Limongan[b]

[a] *Department of Rural Technology, College of Rural Development, Can Tho University, Campus II, 3/2 Street, Ninh Kieu District, Can Tho City 900000, Viet Nam*

[b] *Department of Civil and Construction Engineering, National Taiwan University of Science and Technology, No. 43, Sec. 4, Keelung Rd., Taipei 10607, Taiwan, ROC*

*Author to whom correspondence should be addressed

Tel.: +886 2 27376566; Fax: +886 2 27376606

E-mail: htphuoc@ctu.edu.vn (T.-P. Huynh)

Abstract

Creep and shrinkage behaviors are critical factors in the precast/ prestressed concrete industry because these factors allow engineers to assess the long-term performance of concrete and to develop life-cycle estimates for concrete structures. The current study presents the results of an experimental work that addresses creep and shrinkage behaviors as well as the development of compressive strength in ordinary Portland cement concrete (OPC), high-performance concrete (HPC), and self-consolidating concrete (SCC). The concrete mixtures created for the present study were used to fabricate prestressed bridge girders. A conventional method (ACI) was used to design the mixture proportion for OPC and a densified mixture design algorithm (DMDA) was used to design the mixture proportions for HPC and SCC. All concrete mixtures had the same target strength of 69 MPa (10000 psi) at 56 days. Additionally, a comparative performance in terms of strength development and creep and shrinkage behaviors of ACI and DMDA concrete is performed in the present study. Test results show that all of the samples attained the target strength after 28 days of curing and that the strengths of each continued to increase afterward. Importantly, the incorporation of pozzolanic materials into concrete mixtures affected the propagation of creep strain and shrinkage positively. Furthermore, the DMDA concrete sample delivered better long-term performance than ACI concrete in terms of compressive strength, creep strain, and shrinkage.

Keywords: Creep; shrinkage; high-performance concrete (HPC); self-consolidating concrete (SCC); densified mixture design algorithm (DMDA); compressive strength.

1. Introduction

Today, the global construction industry consumes over 10 billion tons of concrete annually [1]. Over the past decade, in order to meet the requirements of advanced construction activities, the demand specifications for concrete have expanded beyond the traditional considerations of durability, cost, and safety to include considerations of workability and ecology [2]. Traditional concrete uses a relatively high water-to-cement (w/c) ratio as a safety criterion. However, this practice increases the risks of early deterioration, corrosion, and cracks [2–5]. Thus, the water-to-binder (w/b) ratio influences the long-term performance of concrete. High w/b ratios have been associated with increased permeability and increased risks of bleeding and segregation, while the calcium hydroxide ($Ca(OH)_2$) that results from the cement hydration process is a potential cause of sulfate attack, leaching, and precipitation [4–7]. Thus, these problems degrade concrete quality and deteriorate concrete durability. Partially replacing cement with pozzolanic materials such as fly ash (FA), ground granulated blast furnace slag (GGBFS), rice husk ash (RHA), silica fume (SF), and metakaolin (MK) holds the potential to enhance the long-term performance of concrete, as these materials reduce hydration-generated heat and the pozzolanic reaction of these materials turns soluble alkali into C-S-H gel, which is significantly more stable [4,8,9].

Applying a creative densified mixture design algorithm (DMDA) holds promising potential to minimize the abovementioned problems. This algorithm, developed by Hwang's research group at National Taiwan University of Science and Technology (NTUST), has been applied successfully to design concretes that have used in many large projects in Taiwan [10–14]. DMDA effectively reduces both cement and water content using pozzolanic materials and superplasticizer (SP) in order to significantly increase concrete durability. Thus, lower water content reduces drying shrinkage and permeability and lower cement-paste content prevents sulfate attack and alkali-aggregate reactions while reducing hydration heat [15]. Furthermore, the idea of "the least void" is part of the design logic of the DMDA method. Under this idea, pozzolanic materials of particle sizes ranging from micro to nano sizes are used to maximally fill the voids within a concrete structure, with smaller particles may filling the voids between larger particles to create highly compact and dense concrete. Moreover, the comprehensiveness of both the pozzolanic reaction and the filler effect enhances concrete properties [16,17]. Furthermore, partially replacing cement with pozzolanic materials may lower production costs [2], as these materials are often locally available as waste / recycled products or industrial byproducts. Moreover, concrete with good workability requires less labor to use and thus may further reduce the overall costs of construction. Finally, using less cement reduces energy consumption and CO_2 emissions, which reduces the negative impact of concrete production on the environment [4].

Concrete durability is a major concern in construction works. It is known that the volume of concrete changes across its service life. This change is attributable primarily to applied loads and shrinkage [18]. Loaded concrete experiences both instantaneous, recoverable elastic deformation and a slow, inelastic deformation, called creep. The deformations of loaded concrete with and without moisture loss are known, respectively, as drying creep and basic creep. Alternatively, the deformation of unloaded concrete is known as shrinkage. The four principal types of shrinkage are: plastic shrinkage (caused by moisture loss from concrete prior to setting), autogenous shrinkage (caused by self-desiccation during concrete hydration), carbonation shrinkage (resulted from the chemical reactions between hydrated concrete and CO_2 in the air), and drying shrinkage (caused by the long-term dehydration of concrete over an extended period of time). Creep and shrinkage are of crucial importance to the durability, long-term serviceability, long-term stability, and safety of concrete structures. Therefore, many research works have investigated the behaviors of concrete such as increased deflection and curvature, cracking, losses in strength, and the redistribution of prestress and stress that may impact negatively on the viability of concrete structures [19].

Vandewalle [19] studied the issue of concrete creep and shrinkage at cyclic ambient temperatures. Their examination of the effects of weather on cast and loaded concrete, relative humidity (RH), type of cement, and concrete composition found that shrinkage was affected by both weather and humidity, while creep was affected primarily by the weather conditions at the time when the concrete was casted and loaded. Li and Yao's [20] investigation of the effects of ultra-fine GGBFS and SF on the creep and drying-shrinkage characteristics of HPC found that GGBFS/SF-enhanced concrete earned creep and drying-shrinkage values that were significantly lower than traditional high-strength concretes. Nassif et al.'s [21] investigation of the effects of curing method, including air-dry curing, moist curing, and compound curing, on autogenous and drying shrinkage in normal and light-weight HPCs led to the finding that moist curing concrete immediately after finishing improves autogenous-shrinkage performance. Additionally, both FA and lightweight aggregates were found to improve the autogenous shrinkage of concrete with very low w/b ratios. In Zhang et al.'s [22] investigation of autogenous shrinkage in ordinary Portland cement (OPC) and silica-fume (SF) concrete, concrete samples of different w/b ratios (0.26–0.35) and SF contents (0–10% by weight of cement) were prepared. Results found that autogenous shrinkage rose with increasing SF content and a decreasing w/b ratio and that the autogenous shrinkage strains of SF-concrete with low w/b ratios developed more rapidly than the other samples. Lee at al.'s [23] investigation of autogenous shrinkage in concrete samples that were prepared with different w/b ratios (0.27–0.42) and GGBFS contents (0–50%) found that the samples containing GGBFS exhibited larger autogenous shrinkage values than GGBFS-free OPC and that GGBFS content was positively associated with autogenous shrinkage. Soliman and Nehdi [24] investigated the effects of drying conditions on the autogenous shrinkage of ultra-HPC at early-ages by exposing samples to different temperature (10, 20, and 40˚C) and RH (40–80%) conditions. They found that drying conditions significantly affect both early strength development and autogenous shrinkage behavior and that adequate curing is essential to reducing shrinkage in ultra-HPC. Khayat and Long's [25] investigation of the autogenous and drying shrinkage of precast, prestressed SCC and HPC found the 300-day drying shrinkage to be 5–10% higher in the SCC than the HPC, although the autogenous shrinkages for these two types of concrete were similar. Hwang and Khayat's [26] investigation of the effect of mixture design on the restrained shrinkage of SCC samples that were prepared using different w/b ratios (0.35 and 0.42) found that the concrete samples that were prepared with higher w/b ratios exhibited higher drying shrinkage and that SCC concrete had a higher cracking potential than both HPC and OPC due to higher paste content. Güneyisi et al.'s [27] investigation of the development of strength and of the drying shrinkage in SCC containing FA, GGBFS, SF, and MK found that increasing FA content was associated with a slight reduction in compressive strength; that the strength of the GGBFS sample was comparable to that of the control concrete, while those of the SF and MK samples were stronger than the control concrete; and that replacing cement with FA, GGBFS, and MK reduced the drying shrinkage of SCC, while replacing cement with SF increased the drying shrinkage. Finally, Leemann et al.'s [28] investigation of the effects of paste volume and cement type on the E-modulus, flexural and compressive strengths, drying shrinkage, creep, and stress development in SCC found that these two variables affected creep and shrinkage significantly, with the volume of paste related directly and positively to shrinkage levels.

Most previous works focus on evaluating the properties of conventionally prepared Portland cement concrete. Therefore, to address the limited information in the literature on the characteristics of concretes that are designed using DMDA, the present study investigates the long-term performance of DMDA concrete (HPC and SCC) in terms of compressive strength development, creep, and shrinkage as compared to conventional concrete (OPC). Furthermore, the present study compares the effects of the DMDA and ACI mix designs on the long-term performance of these concretes. The results are then applied to the fabrication of prestressed bridge girders.

2. Experimental programs

2.1. Materials

The binder materials used in the present research included: type-I OPC produced by Asia Cement Corporation, class-F fly ash (FA) supplied by Taichung Power Plant, ground granulated blast furnace slag (GGBFS) provided by China Hi-Ment Corporation, and silica fume (SF) produced by Elkem Silicon Materials. Table 1 presents the characteristics of these binder materials. The present study uses natural sand and crushed stone sourced from local quarries in Taiwan as fine and coarse aggregates, respectively, with the physical properties of these aggregates shown in Table 2. A commercially available type-G superplasticizer (SP), containing 43% solid content with a specific gravity of 1.19, was used to obtain the desired workability of the fresh concrete mixture. Domestic, unfiltered tap water that conforms to ASTM C1602 [29] was used as the mixing water.

2.2. Mix design concepts and concrete proportions

The quantity of paste that is used in a concrete mixture greatly affects the performance of the resultant concrete [2,4]. Therefore, performance may be improved by using appropriate amounts of cement, pozzolanic materials, mixing water, and chemical admixture.

In the present study, a traditional ACI mix design method [30] and a DMDA mix design method were used to design concrete ingredient proportions. In the DMDA method, the fluidity and viscosity of the paste was adjusted and balanced by: carefully selecting and proportioning the materials used, limiting the w/b ratio, and adding the appropriate amount of

SP. Furthermore, the different types of concrete (OPC, HPC, and SCC) that were used were designed to achieve the same target strength of 69 MPa (10000 psi) at 56 days. Table 3 shows the mixture proportions by weight of each concrete ingredient. The mixtures "H100" and "S100" were designed using the DMDA method and the control mixture "O100" was designed using the ACI method. A constant w/b ratio of 0.22 was used for all of the concrete mixtures. Hwang's research group has reported the details of the standard procedures for the DMDA mix design and design criteria previously [4,14,15].

2.3. Mixing procedures and samples preparation

The concrete ingredients were mixed in a laboratory pan mixer. All of the binder materials were dry mixed in a mixing pan at a slow rotation speed setting for 1 minute in order to thoroughly disintegrate any clumps in the dry mix and to obtain a uniform powder. A portion of the mixing water and half of the SP were then added gradually into the mixer to disperse the dry powders, producing a viscose paste. Mixing then continued for another 3 minutes on moderate speed setting in order to achieve a homogeneous paste. Next, the natural sand was added into the mixer. Mixing was allowed to continue for an additional 1 minute. Finally, the crushed stone was added into the mixer, followed by the rest of the mixing water and the remaining half of the SP. The mixer was allowed to run for a further 3 minutes in order to obtain a uniform mixture. Once mixing had finished, different sizes of concrete samples were prepared for the tests of compressive strength, drying shrinkage, autogenous shrinkage, carbonation, and creep. All of these samples were de-molded 24 hours after casting and then cured under conditions that were specified for each test, as described in the following section.

2.4. Testing programs

Compressive strength is one of the most important properties of hardened concrete, as concrete is subject to compression in most of structural applications. The compressive strength test used in the present study was conducted in accordance with ASTM C39 [31] in order to analyze the development of compressive strength and to determine the load that was necessary for the creep test. The 100 mm-diameter, 200 mm-length cylindrical concrete samples were prepared for the test in accordance with according to the ASTM C31 [32]. These samples were demolded 24 hours after casting then cured in saturated limewater at the temperature of 23 ± 2˚C until the testing age. Compressive strength values were measured at 3, 7, 14, 28, 56, 91, and 120 days of curing, with the average value of three samples used as the compressive strength value at each testing age.

The autogenous shrinkage test was conducted in accordance with the joint research program format used at Belgian universities [19]. The test was performed using the 100 mm-diameter, 200 mm-length cylindrical concrete samples. The samples were instrumented with two sets of locating-discs that were located on a straight line along the surface of one side of the specimen. The sets were located 10 cm apart from each other and glued to the surface of the specimen using AB-epoxy glue. The concrete samples were coated with epoxy to prevent their interaction / contact with the surrounding environment. These samples were then cured at 23 ± 2˚C and a relative humidity (RH) of 60 ± 4%. Comparator readings for each sample were taken after 1 and 6 hours and then on a daily basis for one week, on a weekly basis for one month, and, finally, at 56, 91, and 120 days.

Drying shrinkage was conducted in accordance with ASTM C157 guidelines [33] using the prismatic samples with dimensions of 75 × 75 × 250 mm. Measurements were made at 1 and 6 hours after demolding and then on a daily basis for one week, on a weekly basis for one month, and, finally, at 56, 91, and 120 days.

The test to determine the depth of the carbonated layer on the surface of hardened concrete was conducted based on the RILEM CPC-18 [34]. A solution of 1% phenolphthalein and 70% ethyl alcohol was used as the indicator. The cubic samples with dimensions of 100 ×

100 × 100 mm were casted and then cured in saturated limewater at 23 ± 2˚C for 28 days. Ambient conditions of roughly 0.03% CO_2, 20˚C, and 65% RH were maintained until testing. The measurement was performed at concrete ages of 28, 56, and 91 days using a digital caliper to an accuracy of 0.01 mm. The average value of three samples was reported for each concrete mixture.

The creep test was conducted for different types of concrete (OPC, HPC, and SCC) in accordance with ASTM C512 [35] using the 100 mm-diameter, 200 mm-length cylindrical concrete samples. The preparation and measurement of creep are shown in Fig. 7. The samples were instrumented with two sets of locating-discs that were located on a straight line along the surface of one side of the specimen. The sets were located 10 cm apart from each other and glued to the surface of the specimen using AB-epoxy glue. Five concrete samples were inserted into each loading frame. These samples were then loaded under a stress-to-strength ratio of 25% of the concrete strength at 28 days of age. A demountable mechanical strain gauge (DEMEC) was used to measure the creep strain. The readings were taken before and after loading and then at 1 and 6 hours afterward, on a daily basis for one week, on a weekly basis for one month, and, finally, at 56, 91, and 120 days.

3. Results and discussion

3.1. Compressive strength

Fig. 1 presents the development of compressive strength in all of concrete samples. Compressive strength generally increased with curing age, which is largely attributable to the pozzolanic reaction [36]. Moreover, Fig. 1 illustrates that ACI concrete (O100) exhibited higher compressive strength values an earlier age (prior to 7 days) than the other types of concrete. However, the compressive strength of DMDA concretes (H100 and S100) was consistently higher than that of ACI concrete after 28 days of curing. This is because at an early age, the pozzolanic reaction in DMDA concrete has not yet become a significant factor in concrete strength, whereas the cement hydration in the ACI concrete has. This further supports that the addition of pozzolanic not only enhances the packing density of concrete but also chemically improves the interfacial transition zone (ITZ) properties through the pozzolanic reaction, contributing to the long-term strength of concrete [4].

On the other hand, the incorporation of SF in the low-w/b concrete was found to be helpful in enhancing compressive strength. This is in good agreement with the experimental results of Johari et al. [37], which found that adding SF to concrete mixtures enhanced concrete strength significantly. As seen in Fig. 1, the compressive strength of concrete samples increased rapidly at an early age, which may be attributed to the combined influence of accelerated cement hydration and the microfiller effect due to the partial replacement of cement with SF [37]. Additionally, the extreme fineness of SF particles provided nucleation sites for the calcium silicate hydrate (C-S-H). Furthermore, the ultrafine SF acts as a microfiller to densify the transition, which improves the matrix-aggregate bond and increases concrete strength [38]. Finally, both of the ACI and DMDA samples reached their target strength of 69 MPa (10000 psi) after only 28 days of curing, rather than after the expected 56 days.

3.2. Autogenous shrinkage

Fig. 2(a) presents the development in autogenous shrinkage (AS) of the ACI and DMDA concrete samples. As indicated by the slope of the AS curves for both types of concrete, the AS developed rapidly at the early ages (prior to 7 days) and slowly at the later ages of concrete. This phenomenon is in line with the result that was reported by Li et al. [39]. The AS values for the OPC, SCC, and HPC at 7 days of age had, respectively, achieved 55.0%, 50.0%, and 58.6% of their final 120-day AS values. At 28 days of age, these values had increased to 70.3%, 75.8%, and 85.7%, respectively. Moreover, as illustrated in Fig. 2(a), the AS of the HPC remained effectively constant after 56 days, while that of OPC and SCC continued to increase at similar rates. As a result, the ACI concrete registered a greater AS value than that of DMDA concrete at all ages. As shown in Fig. 2a, the final AS values for OPC, SCC, and HPC microstrain were 385.5, 350.0, and 279.9, respectively. Thus, the final AS values for SCC and HPC were 90.8% and 71.8% of the AS value for OPC.

Previous research works have reported that concrete with low water-to-cement (w/c) ratios experience faster and greater AS strain than concrete with high-w/c ratios, regardless of concrete type. At lower w/c ratios, concrete mixtures have a higher cement content, which is the major factor, due to hydration-heat and chemical-shrinkage effects, underlying higher AS values [23,39,40]. Additionally, after reacting with cement, some of the water is chemically bound in the hydration products. Chemical shrinkage thus occurs because these hydration products occupy a smaller volume than their reactants. At this moment, if no extra water is added, empty voids are formed in the volume of the hydrated materials. As the water is progressively consumed from smaller pores during the hydration process, water-air menisci are formed, which leads to self-desiccation. Thus, AS is attributable to the buildup of capillary stresses [41,42]. In the present study, the OPC, SCC, and HPC mixtures had respective w/c ratios of 0.25, 0.35, and 0.39 (Table 3). OPC clearly had the lowest w/c ratio and thus the largest AS. In contrast to ACI concrete, DMDA concrete uses more pozzolanic materials in their mixtures, which significantly reduces cement content and increases the w/c ratio, leading to a low AS strain.

On the other hand, the present study used SF as a mineral additive in all concrete mixtures in order to attain the high strength target. As shown in Table 3, ACI concrete contained more SF than the DMDA concrete. This may have led to the greater AS value for OPC, as mentioned previously. Further, the inclusion of SF, an ultrafine powder with high mineral activity and a large surface area, has been reported to refine the pore-size distribution within the concrete. By adding SF to the concrete mixture, the average pore size and porosity of concrete may be reduced while increasing the capillary tension, leading to a higher AS strain [43]. In addition, the high pozzolanic activity of SF increased the self-desiccation effect, leading to an increase in AS [39]. Furthermore, the low AS value that was obtained in the present study is supported by the experimental results of Güneyisi et al. [27], which associated that the increased amounts of pozzolanic materials with reduced shrinkage strain.

3.3. Drying shrinkage

The development of strain over time, as expressed by drying shrinkage (DS), for different types of concrete is shown in Fig. 2(b). As indicated by the slope of the DS curves in Fig. 2(b), the DS of the concretes was somewhat comparable at early ages, while a clear distinction was observed at later ages of the drying period. Although DS takes place over a long period, laboratory results show that around 80% of the DS takes place within about 3 months of casting [44]. Similar to the AS trend, DS in the present study developed rapidly at early ages, but slowed at later ages. For example, the 7-day-old DS values for the OPC, SCC, and HPC were 51.9%, 43.8%, and 38.4%, respectively, of their final, 120-day-old values. By 28 days of age, these values had increased, respectively, to 85.0%, 66.0%, and 75.9%, and continued increasing at a slower rate up to 120 days. In particular, Fig. 2(b) clearly shows that the OPC registered a DS value that was significant higher than those of SCC and HPC under the same curing conditions. Thus, the final DS value measured for OPC was 530.6 microstrain, while the lower DS values measured for SCC and HPC at the same time were 411.2 and 319.2 microstrain, respectively. The final DS values for SCC and HPC were only 75.5% and 60.2% of the DS value for OPC. As previously mentioned, this is attributed to the very low w/c ratio, the high cement content, and the lower mineral admixture content of the OPC mixture, as compared with SCC and HPC. It has been pointed out that the incorporation of GGBFS and SF promotes cement hydration and reacts with CH crystal hydrates, thus increasing the volume of C-S-H gel and the density of the hardened cement paste, which greatly strengthens the structure and reduces the shrinkage of concrete [20]. For the DMDA concrete, SCC a significant higher shrinkage value as compared with that of HPC. This is attributed to the higher volume of paste in the SCC concrete mixture, as supported by Hwang and Khayat [26] and Holt [40].

Aggregate content has been identified as the most important factor that affects shrinkage behavior in concrete because rising aggregate content decreases the shrinkage value [40]. Water content per unit of volumetric concrete is a further important factor affecting the shrinkage behavior of concrete because concrete dehydration during the drying process causes DS. The effects of aggregate and water contents on the long-term DS of both ACI and DMDA concretes are presented in Figs. 3(a) and 3(b), respectively. As expected, DMDA concrete generally exhibits a significantly lower DS value than that exhibited by ACI concrete. The HPC contained the highest aggregate amount and the lowest water content (Fig. 3), reflecting that HPC has the lowest cement paste content of the concrete types examined. Therefore, HPC registered the lowest DS value. It is interesting to note that, in the high-aggregate content concrete, the coarse aggregate particles may have point-to-point contact with each other. Hence, concrete with a stiff-aggregate skeleton will be very effective in resisting stress because aggregate particles cannot be pushed more closely together under the action of interior stress. Additionally, the higher the water content, the more free water that is available within a concrete structure, which leads to an increase in shrinkage strain [45]. As a result, shrinkage strain is dramatically reduced. Experimental measurements conducted in the present study reflect similar results. The effect of aggregate content is somewhat lower, with a decrease of around 10 microstrain for every one percent increase in aggregate content. On the other hand, although OPC has higher aggregate and lower water content than SCC (Fig. 3), SCC earned a significantly lower DS value than OPC. This may due to the advantages of applying DMDA technology to the SCC mixture design, creating a dense concrete structure and thus preventing shrinkage.

3.4. Carbonation

Carbonation is affected by the diffusivity of the hardened cement paste, and the carbonation rate is controlled by the ingress of CO_2 into the concrete pore system through diffusion. This process usually takes a long time due to the very slow speed of diffusion [46]. Papadakis at al. [47] reported a relative humidity of 60–75% as the condition most favorable to carbonation progress. Under this condition, water concentrates on pore walls, creating a hollow center that permits atmospheric CO_2 to enter deeper into pores, where it reacts with the alkalis. On the other hand, Kulakowski et al. [48] pointed to a critical threshold for the carbonation behavior of concrete, delimited by a w/b ratio of 0.45-0.5. Below this range, the porosity of the cementitious matrix is the main determinant of carbonation.

Fig. 2(c) shows the results of carbonation depth measurement on both ACI and DMDA concretes, with carbonation depth increasing with increasing carbonation duration for all concrete mixtures. The rate of increase in carbonation depth is fastest between day 28 and day 56, with lower rates found between day 56 and day 91 (Table 4). Due to the slow pace of the pozzolanic reaction, porosity may be expected to be higher during the initial stage, allowing for a more rapid diffusion of CO_2, which would generate higher carbonation rates [49]. Moreover, Fig. 2(c) shows that the carbonation resistance of DMDA concrete was higher than that of ACI concrete for all accelerated carbonation periods. This may be due to the previously mentioned advantages of the DMDA mix design method. The inclusion of pozzolanic materials in DMDA concrete reduced the depth of carbonation because the pozzolanic reaction and filling effect promote smaller pore sizes and volumes, which reduce the carbonation rate [46]. In addition, Table 4 shows the rate of increase in carbonation to be quite high at the higher level of cement content (O100 mixture), with that rate decreasing with the lower levels of cement content (S100 and H100 mixtures). Khalil and Anwar [50] and Turk at al. [51] reported similar findings. Furthermore, it is suspected that the addition of SF to the concrete samples improved the carbonation resistance during all accelerated carbonation periods. Many researchers [48,50–53] have concluded that including SF may reduce the carbonation depth of concrete. However, SF, as other pozzolanic materials, requires time to react. This delay in the reaction process explains the relatively lower increase between days 56 and 91 in comparison with days 28 to 56.

3.5. Total shrinkage

The total shrinkage (TS) versus the curing age of concrete samples used in the present study is plotted in Fig. 2(d). The TS consists of AS (Fig. 2a) and DS (Fig. 2b). Shrinkage tends to increase at a higher rate at the beginning and then diminishes afterward. Surface tension due to water being expelled from the capillary pores of the hydrated cement paste in early-age cement is largely responsible for this hydraulic shrinkage [54], while later-age shrinkage is largely caused by the loss of water that had absorbed into the surface of the hydrated cement paste [55]. In the present study, the TS values for OPC, SCC, and HPC at 120 days old were 916.1, 761.1, and 596.2 microstrain, respectively. The ACI concrete had a TS that was significantly larger than the DMDA concrete. As the pozzolanic reaction does not occur at an early age, the pore characteristics of the DMDA concrete is governed by the water content in the mix. At later ages, the pozzolanic reaction contributes greatly to reducing the volumes and sizes of pores within concrete. At the same time, evaporation reduces the humidity of concrete to a level that is in balance with the surrounding environment, which was about 60% in the present study. In turn, the depletion of capillary water that causes shrinkage is dominated by self-desiccation. Moreover, SF is believed to affect TS significantly due to the significant influence of SF on AS and DS [43]. Fig. 4 presents the ratio of DS to AS for different concrete types. The result of the present study was similar that of Tazawa and Miyazawa [56] in that the TS becomes more heavily weighted toward AS than DS as the w/c ratio becomes smaller. This means that the TS is fully attributable to autogenous deformation at low w/c ratios. Thus all of the DS that was measured on the concrete samples in this situation would result from AS. Fig. 4 shows clearly that the TS accounted for 60% to 90% of AS in the concrete samples.

3.6. Creep

Creep strain in concrete may affect the performance of concrete structures both positively and negatively. Creep relieves stress concentrations induced by shrinkage, changes in temperature, or the movement of supports. However, creep may be harmful to the safety of the structures. Therefore, it is desirable to limit creep strain as low as possible, especially in prestressed concrete structures. The development of creep strain over time for both ACI and DMDA concretes is presented in Fig 5. Similar to the shrinkage trend, creep strain developed rapidly for all concrete types in early ages and then more slowly in later ages. The ACI concrete samples exhibited higher creep values than the DMDA samples at all concrete ages. As the main difference between DMDA and ACI concrete is the inclusion in the former of pozzolanic materials, it may be logically inferred that pozzolanic materials influence significantly the development of creep strain. This is in line with Massazza [57]. Moreover, the lower creep value for DMDA concrete may be attributed to the denser structure, stronger paste matrix, and improved paste-aggregate interface that is inherent in the DMDA mix design and to the effectiveness of the pozzolanic reaction and the filling effect. This line of reasoning is supported by the findings of Brooks and Johari [58].

The inclusion of SF generally influences the creep strain of concrete. As reported by Brooks [59], at a constant stress-to-strength ratio, the creep strain decreases for SF percentages below 15% and increases at higher percentage levels. Experimental results for the creep strain of the concrete samples in the present study reflected a similar trend in that incorporating SF was associated with reduced creep strain. As noted in previous research, the reduction in creep strain for SF concrete may due to reductions in shrinkage strain and increases in compressive strength [60].

The load-induced, time-dependent deformations of concrete have been widely attributed to: (1) the movement of capillary and adsorbed water within the concrete system, (2) the movement of water into the environment, and (3) the development and propagation of internal micro-cracks. The rate and magnitude of creep strain that is associated with the first two processes depend on the relative volume of pores and spaces that occupy these pores at the time of loading. However, for young concrete, the creep that is due to the latter process may commence relatively earlier for concrete mixtures with lower w/c ratios and thus may exhibit significantly more creep at an early age. This is because water in the capillary pores move initially, followed by the movement of adsorbed water [61]. This may explain why the ACI concrete, with a lower w/c ratio, has a higher creep value than the DMDA concrete.

On the other hand, the effects of aggregate and water content on the creep strain of all of the concrete samples are shown in Figs. 6(a) and 6(b), respectively. Fig. 6(a) shows that lower creep values are attributed to higher aggregate content. Wight and Macgregor [62] reported that applying a load to concrete creates an instantaneous elastic strain that will develop into creep if that load is sustained. Moreover, the magnitude of this creep will be one to three times the value of the instantaneous elastic strain, as it is proportional to the cement paste content and thus inversely proportional to the aggregate volumetric content. Fig. 6(b) shows a trend that runs contrary to Fig. 6(a). Here, higher water content caused greater creep strain in the concrete samples. Water content is a critical factor affecting the development of creep strain [63]. When there is no exchange of water with the ambient environment, the evaporable water content of a concrete sample relates positively to degree of creep, with lower evaporable water content associated with lower creep.

4. Conclusions

The present study investigated the long-term performance of DMDA concrete (HPC and SCC) and conventional ACI concrete (OPC), including the development of compressive strength and creep and shrinkage behaviors. The following conclusions may be drawn from the results of the experiments that were conducted for the present study:

1. The compressive strength of all of the concrete samples increased with curing age. Both DMDA and ACI concretes reached their target strength after 28 days of curing rather than after 56 days, which was the time that was initially estimated. The strength of the samples continued to increase through day 120. The DMDA concrete samples exhibited greater long-term strength than the ACI concrete samples, which is attributed mainly to the pozzolanic reaction and to the filling effect of the pozzolanic materials, which were introduced via the DMDA mix design technology.

2. The incorporation of pozzolanic materials in the DMDA concrete samples positively affected not only the development of compressive strength but also the propagation of creep strain and the shrinkage behavior. In particular, the inclusion of SF in the concrete mixtures enhanced compressive strength and carbonation resistance, increasing AS while reducing DS and creep strain in the samples.

3. Aggregate and water content are two important factors that were found to affect creep strain and shrinkage behavior significantly. Particularly, increasing the aggregate content decreased creep strain and shrinkage in samples, while the opposite trend was observed for samples with higher water contents in their concrete mixtures.

4. The results of the present study support that DMDA concrete delivers better long-term performance than ACI concrete in terms of compressive strength, creep strain, and shrinkage. Therefore, using DMDA mix design technology to densify the pore structure of concrete holds promising potential to further increase concrete strength and to further reduce micro-cracking, creep, and shrinkage.

Acknowledgements

This research was sponsored by the Ministry of Transportation and Communications, Taiwan, under project grant No. 103-521. The authors also appreciate the valuable assistance that was provided by Hwang's research group at the National Taiwan University of Science and Technology (NTUST).

References

[1] Z.J. Li, C. Leung, Y.P. Xi, Structural renovation in concrete, Taylor & Francis, New York, 2009.

[2] P.K. Chang, Y.N. Peng, C.L. Hwang, A design consideration for durability of high-performance concrete, Cement & Concrete Composites. 23 (2001) 375–380.

[3] B. Bissonnette, P. Pierre, M. Pigeon, Influence of key parameters on drying shrinkage of cementitious materials, Cement and Concrete Research. 29 (1999) 1655–1662.

[4] Y.Y. Chen, L.A.T. Bui, C.L. Hwang, Effect of paste amount on the properties of self-consolidating concrete containing fly ash asnd slag, Construction and Building Materials. 47 (2013) 340–346.

[5] N. Su, B. Miao, A new method for the nix design of medium strength flowing concrete with low cement content, Cement & Concrete Composites. 25 (2003) 215–222.

[6] N. Su, K.C. Hsu, H.W. Chai, A simple mix design method for self-compacting concrete, Cement and Concrete Research. 31 (2001) 1799–1807.

[7] P.C. Aïtcin, The durability characteristics of high performance concrete: a review, Cement & Concrete Composites, 25 (2003) 409–420.

[8] A.R. Bagheri, H. Zanganeh, M.M. Moalemi, Mechanical and durability properties of ternary concretes containing silica fume and low reactivity blast furnace slag, Cement & Concrete Composites. 34 (2002) 663–670.

[9] H. Toutanji, N. Delatte, S. Aggoun, R. Duval, A. Danson, Effect of supplementary cementitious materials on the compressive strength and durability of short-term cured concrete, Cement and Concrete Research. 34 (2004) 311–319.

[10] J.C. Chern, C.L. Hwang, D.H. Tsai, Research and development of high-performance concrete in Taiwan, Concrete International. 17 (1995) 1–76.

[11] C.L. Hwang, J.J. Liu, L.S. Lee, F.Y. Lin, Densified mixture design algorithm and early properties of high-performance concrete, Journal of the Chinese Institute of Civil and Hydraulic Engineering. 8 (1996) 217–229.

[12] C.C. Chang, C.L. Hwang, Y.N. Peng, Application of high-performance concrete to high-rise building in Taiwan, Advances in Structural Engineering. 4 (2001) 65–73.

[13] C.T. Tsai, L.S. Li, C.C. Chang, C.L. Hwang, Durability design and application of steel fiber reinforced concrete in Taiwan, The Arabian Journal for Science and Engineering. 34 (2009) 57–79.

[14] T.Y. Tu, Y.Y. Chen, C.L. Hwang, Properties of HPC with recycled aggregates, Cement and Concrete Research. 36 (2006) 943–950.

[15] C.L. Hwang, M.F. Hung, Durability design and performance of self-consolidating lightweight concrete, Construction and Building Materials. 19 (2005) 619–626.

[16] P.K. Chang, An approach to optimizing mix design for properties of high-performance concrete, Cement and Concrete Research. 34 (2004) 623–629.

[17] C.L. Hwang, T.P. Huynh, Investigation into the use of unground rice husk ash to produce eco-friendly construction bricks, Construction and Building Materials. 93 (2015) 335–341.

[18] D.W. Mokarem, R.E. Weyers, D.S. Lane, Development of performance specifications for shrinkage of portland cement concrete, Transportation Research Record. 1834 (2003) 40–47.

[19] L. Vandewalle, Concrete creep and shrinkage at cyclic ambient conditions, Cement & Concrete Composites. 22 (2000) 201–208.

[20] J.Y. Li, Y. Yao, A study on creep and shrinkage of high performance concrete, Cement and Concrete Research. 31 (2001) 1203–1206.

[21] H. Nassif, N. Suksawang, M. Mohammed, Effect of curing methods on early-age and drying shrinkage of high-performance concrete, Transportation Research Record. 1834 (2003) 48–58.

[22] M.H. Zhang, C.T. Tam, M.P. Leow, Effect of water-to-cimentitious materials ratio and silica fume on the autogenous shrinkage of concrete, Cement and Concrete Research. 33 (2003) 1687–1694.

[23] K.M. Lee, H.K. Lee, S.H. Lee, G.Y. Kim, Autogenous shrinkage of concrete containing granulated blast-furnace slag, Cement and Concrete Research. 36 (2006) 1279–1285.

[24] A.M. Soliman, M.L. Nehdi, Effect of drying conditions on autogeous shrinkage in ultra-high performance concrete at early-age, Materials and Structures. 44 (2011) 879–899.

[25] K.H. Khayat, W.J. Long, Shrinkage of precast, prestressed self-consolidating concrete, ACI Materials Journal. 107 (2010) 231–238.

[26] S.D. Hwang, K.H. Khayat, Effect of mix design on restrained shrinkage of self-consolidating concrete, Materials and Structures. 43 (2010) 367–380.

[27] E. Güneyisi, M. Gesoğlu, E. Özbay, Strength and drying shrinkage properties of self-compacting concretes incorporating multi-system blended mineral admixtures, Construction and Building Materials. 24 (2010) 1878–1887.

[28] A. Leemann, P. Lura, R. Loser, Shrinkage and creep of SCC – The influence of paste volume and binder composition, Construction and Building Materials. 25 (2011) 2283–2289.

[29] ASTM. Standard specification for mixing water used in the production of hydraulic cement concrete, C1602. In: Annual book of ASTM standards; 04(02).

[30] ACI. Standard practice for selecting proportions for normal, heavyweight, and mass concrete, 211.1-91. In: American Concrete Institute, US.

[31] ASTM. Standard test method for compressive strength of cylinderal concrete specimens, C39. In: Annual book of ASTM standards; 04(02).

[32] ASTM. Standard practice for making and curing concrete test specimens in the field, C31. In: Annual book of ASTM standards; 04(02).

[33] ASTM. Standard test method for length change of hardened hydraulic cement mortar and concrete, C157. In: Annual book of ASTM standards; 04(02).

[34] RILEM. Measurement of hardened concrete carbonation depth, CPC-18. RILEM Publications SARL.

[35] ASTM. Standard test method for creep of concrete in compression, C512. In: Annual book of ASTM standards; 04(02).

[36] C.L. Hwang, T.P. Huynh, Evaluation of the performance and microstructure of ecofriendly construction bricks made with fly ash and residual rice husk ash, Advances in Materials Science and Engineering. 2015 (2015).

[37] M.A.M. Johari, J.J. Brooks, S. Kabir, P. Rivard, Influence of supplementary cementitious materials on engineering properties of high strength concrete, Construction and Building Materials. 25 (2001) 2639–2648.

[38] R.J. Detwiler, P.K. Mehta, Chemical and physical effects of silica fume on the mechanical behavior of concrete, ACI Materials Journal. 86 (1989) 609–614.

[39] Y. Li, J. Bao, Y. Guo, The relationship between autogenous shrinkage and pore structure of cement paste with mineral admixtures, Construction and Building Materials. 24 (2010) 1855–1860.

[40] E.E. Holt, Contribution of mixture design to chemiocal and autogenous shrinkage of concrete at early ages, Cement and Concrete Research. 35 (2005) 464–472.

[41] P. Lura, O.M. Jensen, K. van Breugel, Autogenous shrinkage in high-performance cement paste: An evaluation of basic mechanisms, Cement and Concrete Research. 33 (2003) 223–232.

[42] M. Wyrzykowski, P. Lura, F. Pesavento, D. Gawin, Modeling of water migration during internal curing with superabsorbent polymers, Journal of Materials in Civil Engineering. 24 (2012) 1006–1016.

[43] J.J. Brooks, J.G. Cabrera, M.A.M. Johari, Autogenous shrinkage of concrete, E & FN Spon, London, 1999.

[44] E.E. Holt, Early age autogenous shrinkage of concrete, Technical Research Centre of Finland, Espoo, Finland, 2001.

[45] X.C. Pu, Super-high-strength high performance concrete, Taylor & Francis, New York, 2012.

[46] J.M. Chi, R. Huang, C.C. Yang, Effects of carbonation on mechanical properties and durability of concrete using accelerated testing method, Journal of Marine Science and Technology. 10 (2002) 14–20.

[47] V.G. Papadakis, C.G. Vayenas, M.N. Fardis, Physical and chemical characteristics affecting the durability of concrete, ACI Materials Journal. 88 (1991) 186–196.

[48] M.P. Kulakowski, F.M. Pereira, D.C.C. Dal Molin, Carbonation-induced reinforcement corrosion in silica fume concrete, Construction and Building Materials. 23 (2009) 1189–1195.

[49] P. Sulapha, S.F. Wong, T.H. We, S. Swaddiwudhipong, Carbonation of concrete containing mineral admixtures, Journal of Materials in Civil Engineering. 15 (2003) 134–143.

[50] E.A.B. Khalil, M. Anwar, Carbonation of ternary cementitious concrete systems containing fly ash and silica fume, Water Science. 29 (2015) 36–44.

[51] K. Turk, M. Karatas, T. Gonen, Effect of fly ash and silica fume on compressive strength, sorptivity and carbonation of SCC, KSCE Journal of Civil Engineering. 17 (2013) 202–209.

[52] C.D. Atis, Accelerated carbonation and testing of concrete made with fly ash, Construction and Building Materials. 17 (2003) 147–152.

[53] Q.L. Wang, J.C. Bao, Effect of silica fume on mechanical properties and carbonation resistance of concrete, Applied Mechanics and Materials. 238 (2012) 161–164.

[54] W.F. Perenchio, The drying shrinkage dilemma, Concrete Construction – World of Concrete. 42 (1997) 379–383.

[55] L.M. Dellinghausen, A.L.G. Gastaldini, F.J. Vanzin, K.K. Veiga, Total shrinkage, oxygen permeability, and chloride ion penetration in concrete made with white Portland cement and blast-furnace slag, Construction and Building Materials. 37 (2012) 652–659.

[56] E. Tazawa, S. Miyazawa, Experimental study on mechanism of autogenous shrinkage of concrete, Cement and Concrete Research. 25 (1995) 1633–1638.

[57] F. Massazza, Pozzolanic cements, Cement & Concrete Composites. 15 (1993) 185–214.

[58] J.J. Brooks, M.A.M. Johari, Effect of metakaolin on creep and shrinkage of concrete, Cement & Concrete Composites. 23 (2001) 495–502.

[59] J.J. Brooks, Elasticity, creep, and shrinkage of comcrete containing admixtures, Special Publication. 194 (2000) 283–360.

[60] W.A. Al-Khaja, Strength and time-dependent deformations of silica fume concrete for use in Bahrain, Construction and Building Materials. 8 (1994) 169–172.

[61] M. Smadi, F.O. Slate, A.H. Nilson, Shrinkage and creep of high-, medium-, and low-strength concretes, including overloads, ACI Materials Journal. 84 (1987) 224–234.

[62] J.K. Wight, J.G. MacGregor, Reinforced concrete: mechanics and design, Pearson Education Inc., US, 2009.

[63] Z.P. Bažant, A.A. Ashgari, J. Schmidt, Experimental study of creep of hardened Portland cement at variable water content, Matériaux et Construction. 9 (1976) 279–290.

Table 1

Characteristics of binder materials.

Binder material		OPC	FA	GGBFS	SF
Specific gravity		3.15	2.29	2.91	2.21
Chemical composition (wt.%)	SiO_2	20.04	64.01	35.64	97.65
	Al_2O_3	4.24	22.14	11.25	0.70
	Fe_2O_3	3.12	5.64	0.48	0.05
	CaO	62.43	2.75	41.00	0.35
	MgO	4.17	0.92	6.45	0.42
	SO_3	2.97	0.61	0.90	0.27
	K_2O	0.43	1.36	0.62	0.29
	Na_2O	0.33	0.85	0.29	-
	TiO_2	0.62	0.98	1.26	-
	P_2O_5	-	0.30	-	-

Table 2

Physical properties of fine and coarse aggregates.

Aggregate type	Maximum diameter, mm	Density (OD), kg/m^3	Density (SSD), kg/m^3	Absorption capacity, %	Fineness modulus (FM)	Unit weight, kg/m^3
Natural sand	4.75	2640	2680	1.2	3.02	-
Crushed stone	12.5	2670	2690	0.7	4.31	1648

Table 3

Concrete mixture proportions.

Sample code	W/B	W/C	Concrete ingredient proportion, kg/m^3							
			Cement	GGBFS	FA	SF	Stone	Sand	Water	SP
O100	0.22	0.25	665.2	-	-	73.9	897.5	610.8	163.0	7.4
S100		0.35	517.6	221.9	50.4	50.4	727.7	660.2	181.0	6.5
H100		0.39	336.2	144.1	51.2	62.6	903.5	792.3	130.7	7.1

Table 4

Rate of carbonation increase for different types of concrete.

Sample code	Carbonation depth (mm)			Increase (%)	
	28-day	56-day	91-day	28- to 56-day	56- to 91-day
O100	3.53	4.17	4.31	18.1	3.4
S100	3.38	3.68	3.82	8.9	3.8
H100	3.14	3.39	3.52	8.0	3.8

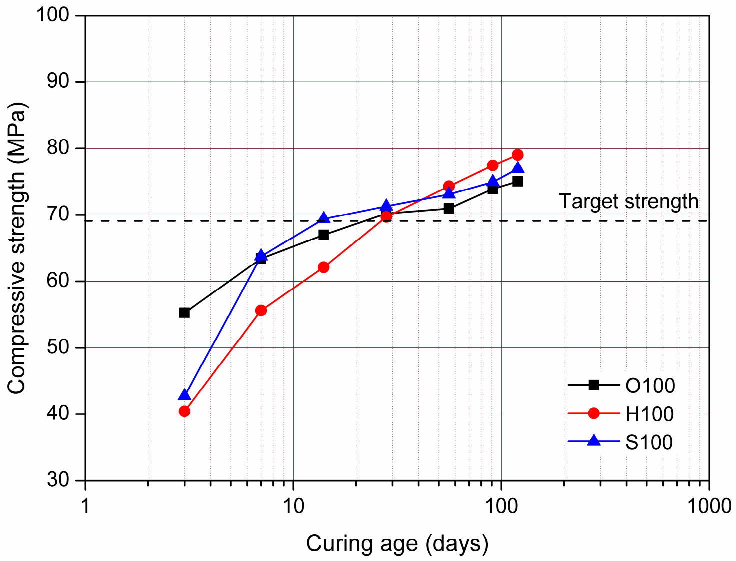

Fig. 1. Development of compressive strength in the concrete samples.

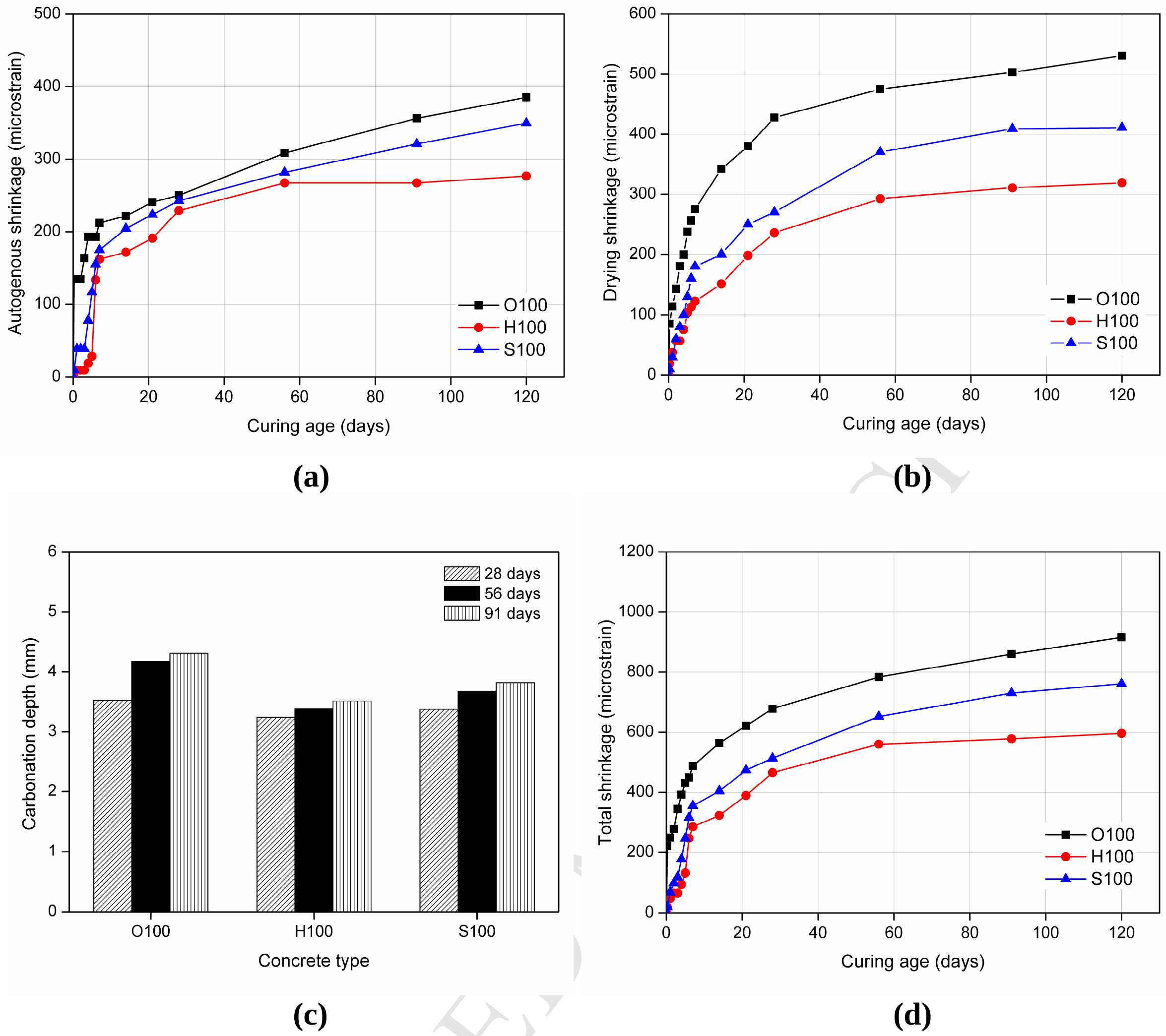

Fig. 2. Development of shrinkage in the concrete samples: (a) autogenous shrinkage; (b) drying shrinkage; (c) carbonation; (d) total shrinkage.

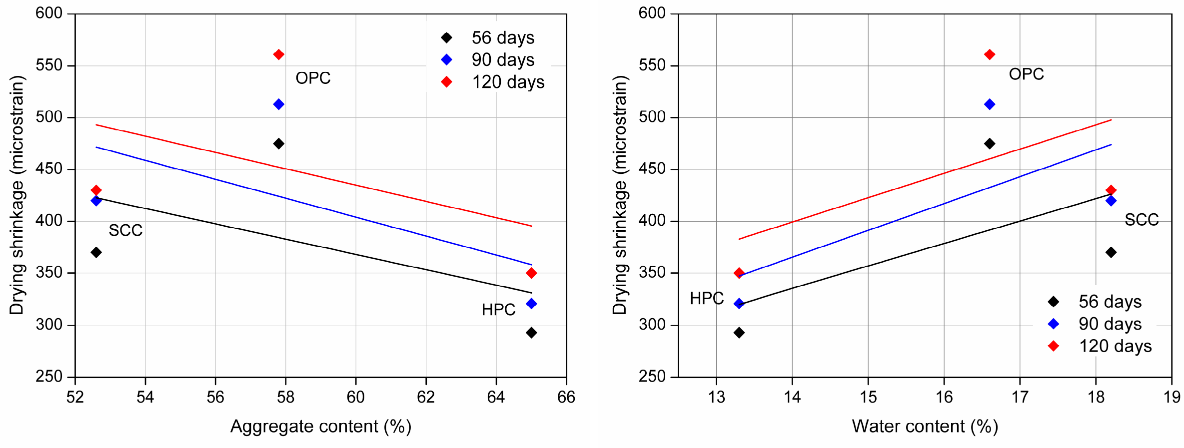

(a) **(b)**

Fig. 3. Effects of (a) aggregate content and (b) water content on drying shrinkage of concrete samples.

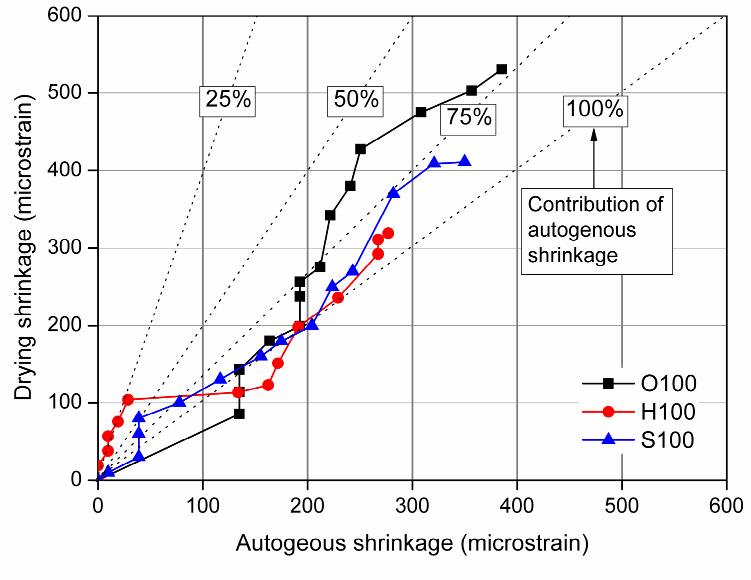

Fig. 4. Ratio of drying shrinkage to autogenous shrinkage in concrete samples.

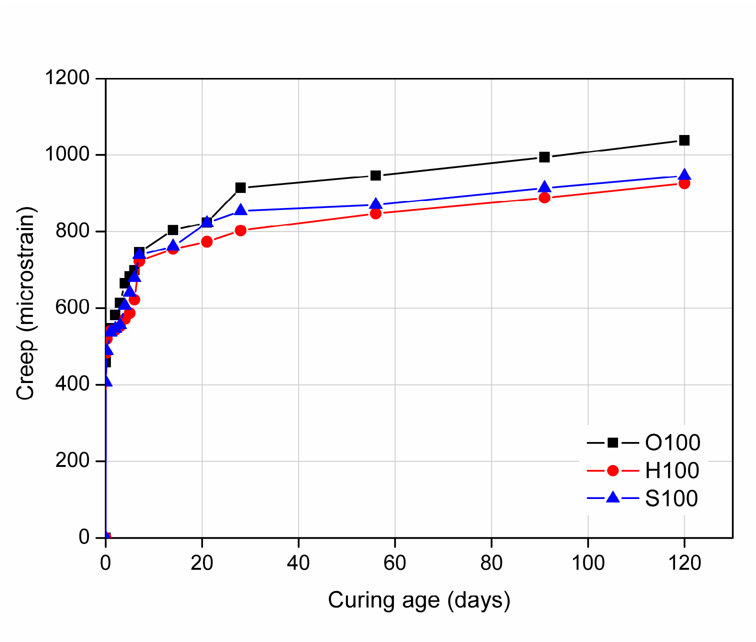

Fig. 5. Development of creep in concrete samples.

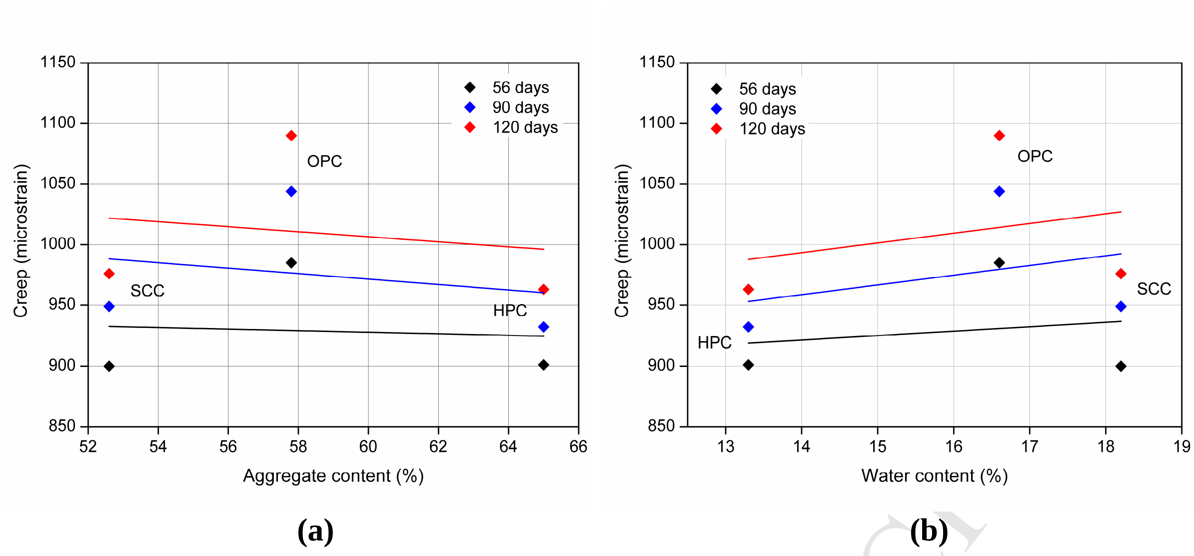

Fig. 6. Effects on creep of (a) aggregate content and (b) water content in concrete samples.

(a) (b) (c)

Fig. 7. Creep setup and measurement: (a) creep specimen and demountable mechanical strain gauge (DEMEC); (b) loading frame with creep specimen; (c) measurement of creep values.